

# 3D imaging of a nuclear reactor using muography measurements with Micromegas detectors

Baptiste Lefevre<sup>1,\*</sup>, Héctor Gomez<sup>1</sup>, Sébastien Procureur<sup>1</sup>, David Attié<sup>1</sup>, Laurent Gallego<sup>2</sup>, Philippe Gonzales<sup>3</sup>, Marion Lehuraux<sup>1</sup>, Bertrand Lesage<sup>4</sup>, Irakli Mandjavidze<sup>1</sup>, Philippe Mas<sup>1</sup>, Daniel Pomarede<sup>1</sup>

<sup>1</sup>CEA/DRF/Irfu, France

<sup>2</sup>CEA/DES/DDSD, France

<sup>3</sup>Assystem Engineering and Operation Services, France

<sup>4</sup>SOM-LIGERON, France

(\*) [baptiste.lefevre@cea.fr](mailto:baptiste.lefevre@cea.fr)

**Abstract**—Transmission muography is a non-invasive and non-destructive imaging method which allows to estimate the integrated density of a volume in a given direction (also referred as opacity). It relies on a reconstruction of muons tracks that crossed the studied volume compared to the corresponding open sky expectation. The experimental setup of the muography developed at CEA Irfu consists in portable muon telescopes. Each of these instruments has four Micromegas gaseous detectors, power and acquisition electronics, and an embedded computer connected to the network allowing remote control. It is then well adapted to deploy them in constrained environments. A muography measurements campaign has been carried out in the decommissioned nuclear reactors G2 and G3 at CEA Marcoule (France) which are expected to be dismantled. We were able to conduct 2D muographies and 3D analyses of inside G2's airtight concrete chamber. In this paper we describe the measurement protocol at the G2 and G3 reactors. We explain what was developed to improve the measurements between G2 and G3 campaigns. It shows how potential improvements were identified in the proof of concept and why we expect a better reconstruction for G3. Among the improvements, we describe how simulations prior to the measurements, denoising and in general automation play an important role to have a precise 3D image in reasonable time.

**Keywords**—Muography, nuclear reactor dismantling, 3D imaging.

## I. INTRODUCTION

MUOGRAPHY is a non invasive and non destructive imaging method that allows, under certain conditions, to estimate the densities inside a targeted volume. Muography is very penetrative compared to other techniques like X-rays and ultrasounds which are rapidly stopped by dense material like metal or concrete. Muography uses the natural muon flux on the contrary of X-rays or neutrography which needs radioactive sources.

2D and 3D non destructive analyses with muography are particularly interesting in constrained environments or on very opaque solids. Muography has been used in archaeology to search for hidden chambers in the Khufu's pyramid [1,2], in

geophysical sciences to monitor volcanoes [3], in homeland security [3] and is currently used in many projects in the nuclear field.

Multiple techniques have been developed and can rely either on small deviations of the muons, or on their absorption or transmission [4]. Among those methods we will focus on transmission muography, which needs to place detectors underneath the studied volume. The muon flux, naturally generated in the atmosphere and mostly vertical will cross the studied volume before it reaches the detectors. Because the number of muons stopped is strongly correlated with the matter density, the volume density “shadow” will be projected on the detectors.

In each direction, this shadow represents the integrated density on a line and is called the opacity noted  $o$  as in (1), where  $\rho$  is the density integrated on the distance  $dl$ .

$$o = \int \rho \cdot dl, \quad (1)$$

Equation (1) can also be written in a vectorial form which is easier to implement in a program. To do so, the volume to image is modeled by voxels (3 dimensional pixels). In (2),  $o$  is the opacity of a line going though the volume,  $\vec{A}$  is the vector of distances traveled in voxels by the line and  $\vec{\rho}$  is the vector of densities of the voxels.

$$o = \vec{A} \cdot \vec{\rho}, \quad (2)$$

Equations (1) and (2) are defined in [5] and used in [6].

Therefore, a muography is firstly represented as a 2D image, where each pixel counts the number of incoming muons for a given direction as in Fig. 1. This muography is then compared with a simulation of the muons expected for each direction in open-air conditions, so it is possible to compute an opacity image. On the opacity image, each pixel represents the integrated density for the studied direction as in Fig. 2.

To produce such images, multiple types of detectors exist. Emulsion films are sensitive to muon hits and are developed afterwards, scintillators work in real time and directly give pixelized images, whereas gaseous detectors work in real time and measure on copper strips the energy deposit induced by the gas ionization.

The muography team at CEA Irfu has developed muon telescopes composed of 4 Micromegas gaseous detectors [7].

These detectors use an Argon-based mixture and high voltages to detect the ionizations that charged particles create in gases. The electrons detached from gas atoms are accelerated and create a cascade that deposit signal on a readout plane. To increase the spatial resolution with less electronics, we use genetic multiplexed Micromegas [8]. The signal's amplitude is measured and analyzed in real time to trigger and store muon-candidate events. The electronic is controlled by an embedded computer in order to have an autonomous and remotely controllable system.

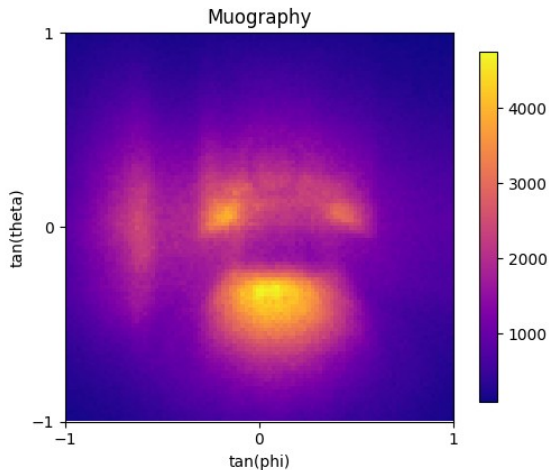


Fig. 1. Muography from below the charging block of the G3 reactor in Marcoule. Each pixel is a direction in space. The scale indicates the number of muons coming from the targeted direction. Orange to yellow pixels are the direction where the muon flux is the highest.

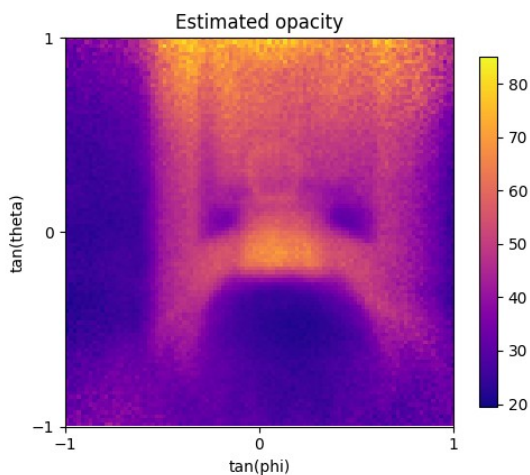


Fig. 2. Computed opacity ( $\text{g}/\text{cm}^2$ ) from below the charging block of the G3 reactor in Marcoule. The opacity is the result of a comparison between the muography of Fig. 1 and an open-sky simulation. The most opaque areas (orange to yellow) show the concrete shielding of the reactor, the charging block and some graphite.

On the telescope, the embedded computer is in charge of maintaining the 4 detectors in condition of operation and of doing some of the preprocess steps. Among those steps, the detector data has to be demultiplexed in order to recover the position of the muon. This step is still subject to new developments which involve machine learning [9].

As it will be described later, the telescopes (composed of 4 Micromegas detectors) are very portable, which makes it possible to do muographies from multiple points of view of the same object, allowing to run 3D analyses by combination of muographies. Whereas the opacity measured in one muography only gives the sum of the densities in one direction, it might be possible to estimate separately all those densities.

## II. G2G3 PROJECT

The G2 and G3 reactors in Marcoule were the first french nuclear reactors connected to the grid. Both are UNGG type reactors (Natural Uranium, Graphite, Gas) and were started in 1958 and 1959 [10]. They worked respectively until 1980 and 1984, producing electricity and plutonium during more than 20 years. After their shutdown, the combustible and most of the supporting functions around the reactor were dismantled. Since 1996, G2 and G3 are monitored and maintained safe, before the full dismantling planned in the next decades.

In the context of this monitoring, the muography was foreseen to conduct a characterization of the reactors. The goals of the team in charge of the monitoring and dismantling (CEA DES/DDSD) are described in [10] : “compare the internal structures [...], characterize the civil engineering [...] and identify potential anomalies”.

The project was launched in 2017 and started with simulations. Whereas X-ray and ultrasounds were not enough penetrative, the simulations demonstrated that the reactor could be imaged by muography.

It was decided to conduct a measurement campaign with telescopes under G2 as a proof of concept.

The complete telescopes weight around 40 kg, measure  $60 \text{ cm} \times 60 \text{ cm}$  and are 1 m high, one of them is shown on Fig. 3. It makes them very portable which allows to do multiple muographies with simple logistic.

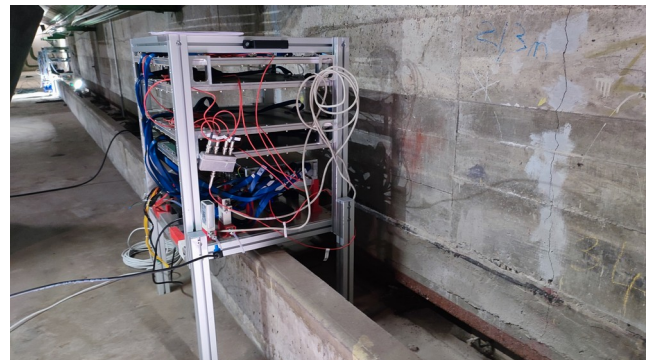


Fig. 3. Muon telescope under the G3 reactor in Marcoule. The cubic telescope is mounted on 4 extension feet to step over a small wall.

Four telescopes were deployed at G2 during the first campaign. On site, the telescopes only need power, gas (a non inflammable Argon-based mixture) and to be connected together with a network router. The G2 G3 site operators were able to place, displace and setup the telescopes, whereas the data taking was controlled remotely by the CEA Irfu team.

This data taking procedure minimizes the intervention time on-site. This is only required to displace the telescopes and if possible to check on the gas consumption. All the data taking is already remotely handled. Ultimately, in more constrained or more radiating environments, our telescopes could be installed on a robot to avoid manual displacements.

Each of the 4 Micromegas on a telescope gives a hit position. With multiple hits we can reconstruct the original track of the muon. In the typical situation described in Fig. 4 the hits are not perfectly aligned. In the following analysis we will be interested in the track direction and the intersection between the track and the bottom Micromegas (called the XOY0 point).

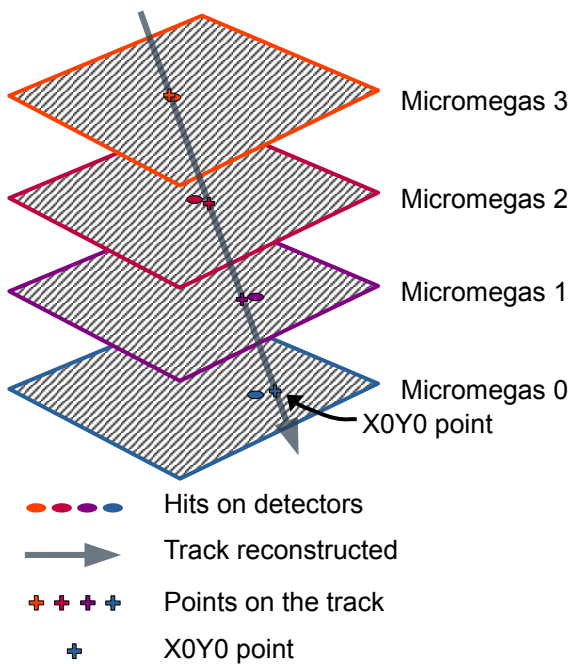


Fig. 4. Drawing of 4 Micromegas detectors with hits (colored points). A track is then reconstructed (gray arrow). The track crosses the detectors on slightly different points (colored crosses). The point on the lowest detector is called XOY0 (blue cross).

### III. MEASUREMENTS

The first measurement campaign (dedicated to the G2 reactor) was a proof of concept of the methodology to manage the telescopes, take data, and do the 3D analysis.

To estimate the densities inside the reactor, it is necessary that the same regions in space are observed from different points of view. For practical reasons, it was decided to use only four telescopes like the one on Fig. 2. but to displace them to different positions. Once they are in position they can be remotely controlled over a secured network connection. In-person operation was only needed to displace the telescopes, once a month in general.

The remote controlling also allowed to have the muographies in real time during the campaign. With all the G2 muographies ready, we worked on a proof of concept of 3D reconstruction [6]. The idea is to use the SART algorithm to solve the ill-posed algebraic problem coming from the

generalization of the formula (2). In (3), multiple rays in space are studied at the same time. The opacity is now a vector  $\vec{\sigma}$ ,  $A$  is the matrix of distances crossed in voxels by rays and  $\vec{\rho}$  is still the vector of the voxel's opacities.

$$\vec{\sigma} = A \cdot \vec{\rho}, \quad (3)$$

The experience acquired during the G2 campaign and the results of SART have been taken into account to define goals and potential improvements for the G3 campaign.

Firstly a new goal was to focus on the analysis of the graphite core because a small displacement of this part of the reactor was suspected. For this purpose we adapted the telescope's positions with simulations of a simplified graphite core.

Secondly, to adapt the telescopes to the G3 constraints we had to build new mechanical parts that facilitated the orientation of the telescopes in narrow spaces like on Fig. 5. With the compact mechanic illustrated below, we were able to place telescopes in narrow corridors at high angles to observe our targets.

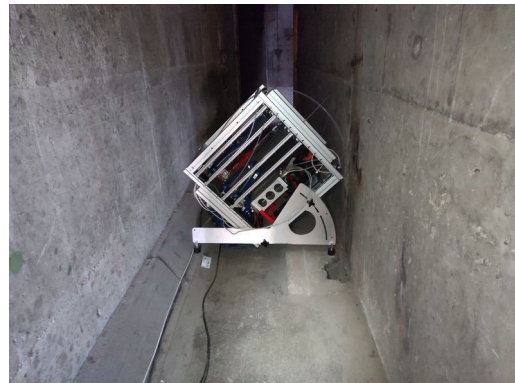


Fig. 5. Muon telescope oriented at 45° in a 1 m large corridor. We recognize the telescope of Fig. 3 but mounted on rotation plates instead of its feet.

Finally we focused on the improvement of the muographies themselves. Indeed the noise present on them tends to be propagated in 3D and has a major effect during the densities estimation with the SART algorithm. Whereas the denoising was a very time consuming task for G2's reconstruction, we discuss here an automatic method and describe its performance.

The improvement of the muographies is also possible with a better positioning of the particle hits on the detector. This step is linked to the detector demultiplexing, which made progress thanks to machine learning [9], but will not be discussed in this paper.

### IV. RESULTS

#### A. Preliminary simulations for the graphite core

In order to focus the analysis on G3's graphite core we did preliminary simulations to compare different scenario and optimize the reconstruction with a given amount of measurement time.

For graphite core, we were wondering if it was better to keep the telescopes longer on a small amount of positions or to

do more positions with less statistics. To arbitrate this trade-off between number of positions and statistical significance we studied 8 scenarios with 4 telescopes available for 2 months. They are illustrated in Fig. 6 and described in Table I.

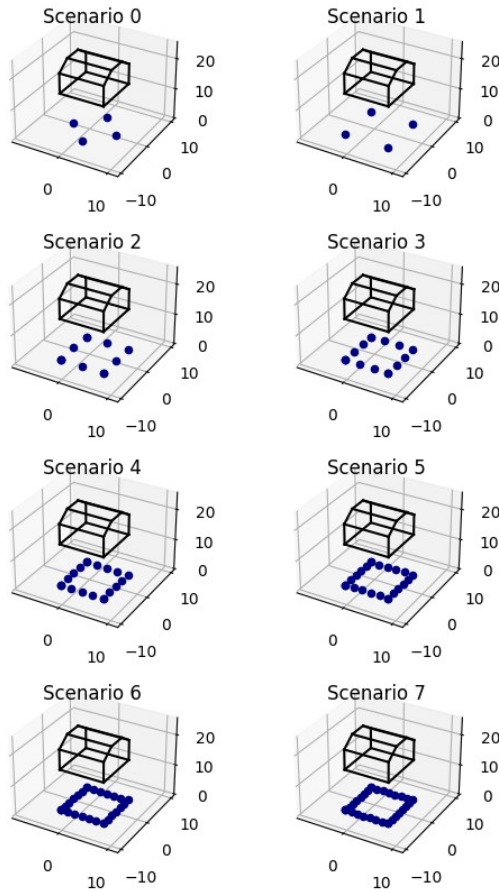


Fig. 6. Illustration of the 8 scenarios where the blue points represent the position of the telescopes under the shape of the graphite core.

TABLE I  
SCENARIOS FOR A 2-MONTHS STUDY OF THE GRAPHITE CORE

Scenario	Number of positions	Duration per position (days)	Position below the graphite core
0	4	60	* Under each face's center
1	4	60	* Under each corner
2	8	30	* Corners * faces centers
3	12	15	* Corners * 3 positions per face
$N \in [4,7]$	$N * 4$	$60 / (N+1)$	* Corners * $N$ positions per face

Every scenario is associated with a number and describe where (and how long) to put the 4 telescopes. The two first scenarios focus on 4 positions only (1 position per telescope). The other scenarios distribute the telescopes under the faces as illustrated in Fig. 6.

For each of these 8 scenarios, we simulated what muographies would be with the graphite core alone, which has a cubic shape with 2 big chamfers on the top as illustrated on Fig. 6.

To understand the trade-off between the number of positions and their duration, the effect of the measurement

time increase may be seen on Fig. 7 where a position under a corner of the graphite core was simulated for 1, 5 and 25 days.

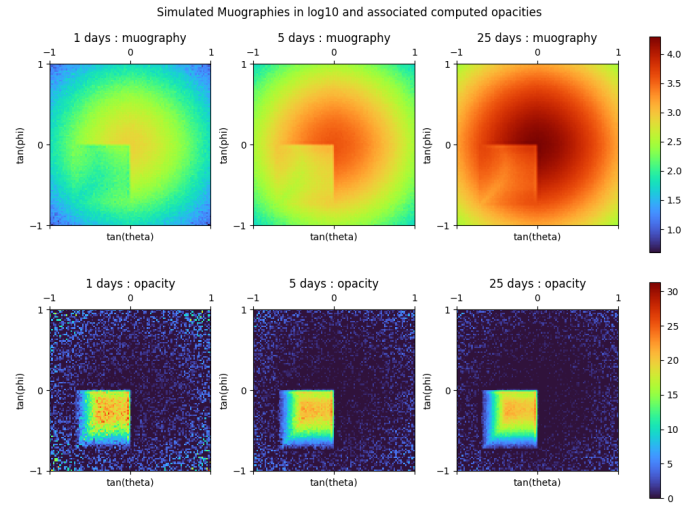


Fig. 7. Simulated muography under a corner of the graphite core for 1, 5 and 25 days. The second row shows the associated computed opacity ( $\text{g}/\text{cm}^2$ ) matrices. We show that the increase of muon number in the muography induce a decrease of noise in the opacity.

On the muographies in Fig. 7, the distributions of muons stay the same when the number of muons increase linearly during time. This increase has few effect on the center of the image because muons are already statistically enough. However, on the edges of the image the opacity calculation needs longer simulations because there are less muons. Moreover the overall opacity image is less noisy with a longer muography.

To sum up, if we do less positions, the muographies will have more statistics which implies that the estimated opacity will be less noisy and significantly better on the edges.

To study the trade-off we ran the simulations mentioned in Table I and ran 3D reconstructions with the SART algorithm. We obtained the integrated densities displayed in Fig. 8. To simplify the visualization, only the pixel above 50% of the maximum of each image are displayed. The last row is the geometry used to run the simulation, ideally the projected densities should have the same shape and value.

Those simulations and reconstructions show that, even if the statistic is lower on each muography, the reconstruction is better with more positions. The improvement is visible on 3 different aspects: the overall shape of the graphite core is more correct, the density estimated in the graphite is more homogeneous and the density value is closer from the expected graphite density.

However we can see that the shape is still suffering some artifacts on the sides and below the core. Moreover the density value is underestimated.

### B. Positions chosen at G3

Even if the best case simulated involves moving the telescopes every 7 days, 16 measurements of 14 days each were carried out for practical reasons. After those measurements, the telescopes were spread on 30 other positions to scan a wider range of the reactor.

The main limitation to the number of positions was that each displacement needed the intervention of the team on site.

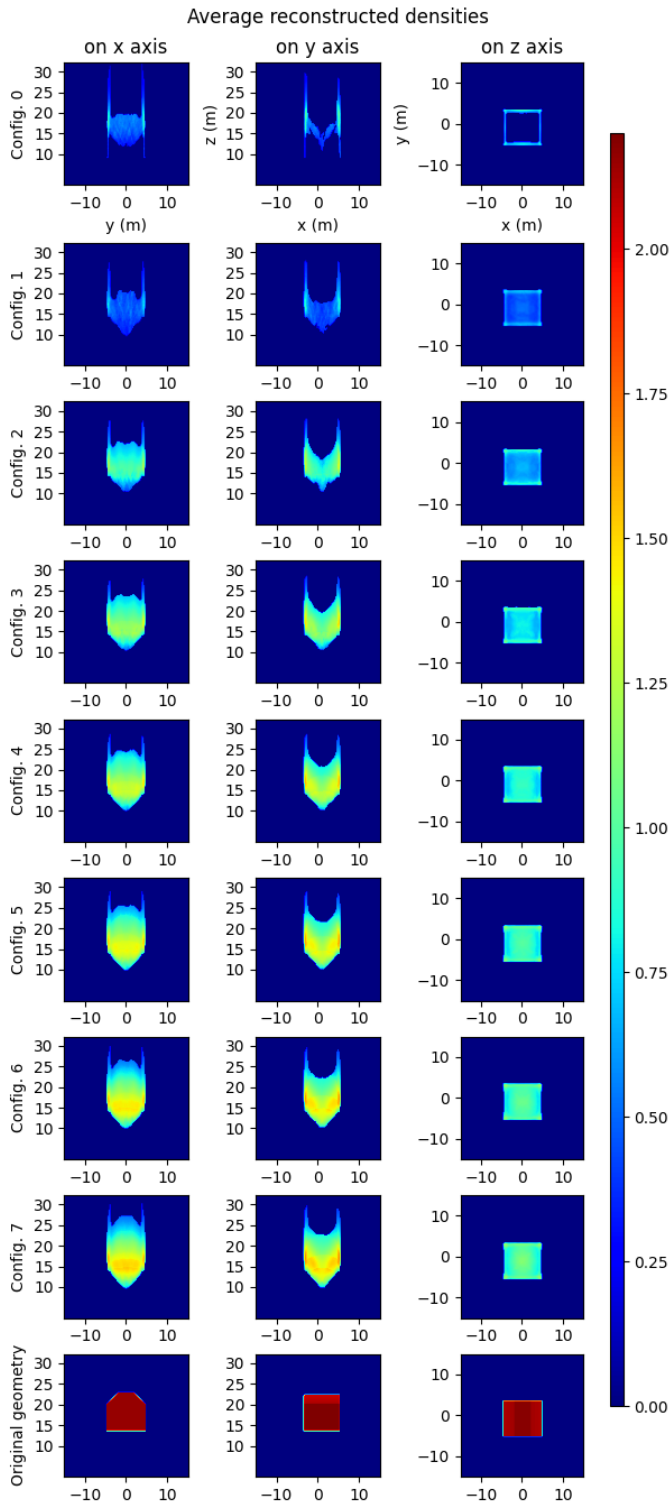


Fig. 8. Eight different scenarios results compared to the real volume simulated (last row). The columns are respectively the average density ( $\text{g/m}^3$ ) of the shape in the x, y and z axis. The common color scale shows the inhomogeneities inside the reconstructed volumes.

In one year of acquisition we were able to realize 46 positions, meaning that each of the four telescopes was moved

in average every month. In comparison, the G2 reconstruction in [6] uses only 27 positions from data taken in 2 years.

The 46 positions at G3 are displayed on Fig. 9 with the shape of the concrete cylinder which contains the graphite core.

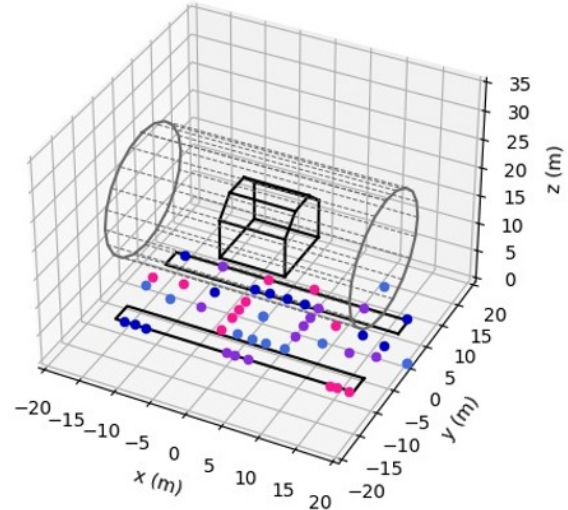


Fig. 9. Map of the 46 positions at G3. The reactor is the cylinder represented in gray. It contains the graphite core represented in black. On the ground 2 black rectangles represent the footprint of the reactor.

We recognize the 16 positions under the graphite core edges. Also most positions are directly under the concrete cylinder. Some positions are outside the cylinder footprint (represented by black rectangles on the ground) in narrow corridors along the reactor as on Fig. 5.

Given the amount of positions, the data preparation before the reconstruction plays a major role. During the G2 campaign most steps of the analysis were separated scripts using different configuration files and had to be started independently. This procedure was revealed not optimal to have results rapidly.

### C. Improvement on muography processing

For G3 we standardized our tools in the form of C++ source codes wrapped into Python libraries thanks to Cython. With this method, the core of our analysis is efficient C++ using the CERN's Root library. But the usage benefits of Python's simplicity and allows to write scripts to automatically analyses the amount of data we produce.

Among the tasks that we wanted to automate, the noise detection and the consequent denoising are very important. Indeed, noise in a muography reconstructs fake muons. If there is an excess of muons in one direction, the opacity calculation will result in an under-estimated value. Indeed, more muons means that the direction is easier to cross for the muons, which means that the opacity is lower. Those under-estimated spots will then be propagated in 3 dimensions by the SART algorithm.

To denoise the muographies without signal loss, we propose a method using some properties of the reconstructed muon tracks. When the Micromegas detectors are subject to noise,

signal appears on some detectors spontaneously on specific spots. If the signals on the detectors are not aligned in space, no track can be reconstructed and the event is dropped. However some of these spots may be enough aligned to be considered as muon tracks. In that case, the tracks connecting the same noisy spots will be close in space.

Tracks close in space will have the same direction and show up as points on the muography like in Fig. 10. But tracks close in space will also have close points of intersection on each planes. We will note  $(X_0, Y_0)$  the points of intersection between the tracks and a virtual plane on the lowest Micromegas. Those points can be used to construct what we call the X0Y0 histogram.

In previous works, ad-hoc conditions were found for each noisy position. To tackle this problem for the G3 analysis, every run of data will be subject to the same test during the track reconstruction step (the 46 positions produced more than 200 runs of data). Firstly the X0Y0 histogram of the studied run is realized with 1 mm large bins. This allows to see in which regions of the telescope the muons are estimated to cross the bottom detector. On this histogram we apply a blurring with a  $5 \times 5$  matrix. After this blurring we consider empirically that pixels above 3.5 times the average are regions of space with noise. We can then select the events crossing this region of the bottom detector.

As an example, the Fig. 10 shows a 5-weeks muography and the associated X0Y0 histogram.

The muography is subject to noise with directions that counts more than 10k muons. When we look at the X0Y0 histogram we see that a pixel at the bottom right is concentrating 10 times more events than the average, it can be filtered to denoise the muography. During the analysis this X0Y0 histogram has  $500 \times 500$  bins in order to select precisely the areas to filter. When applied with the parameters described above,  $50 \text{ mm}^2$  (0.0002 % of the detector) was banned. It deleted around 50k events (0.005% of the events) and gave the result presented in Fig. 1.

This denoising is a necessary step in order to recover the exploitable data from the detector noise. Because this noise is easily recognizable from the exploitable data, we consider it as “visible noise”. Therefore we measured qualitatively the effect of this denoising method as reported in Table II.

No effect on visible noise	Partial cleaning on visible noise	Complete cleaning of visible noise
19 %	37 %	44 %

Results of the described denoising on the visible noise.

In nearly 45% of the noisy positions this methods corrects the visible noise. In the other case it cleans partially the muography, and in less than 20% of the cases it does not detect the noise. Fortunately this method still have improvement potential like a better smoothing and a smarter choice of threshold to determine noisy bins.

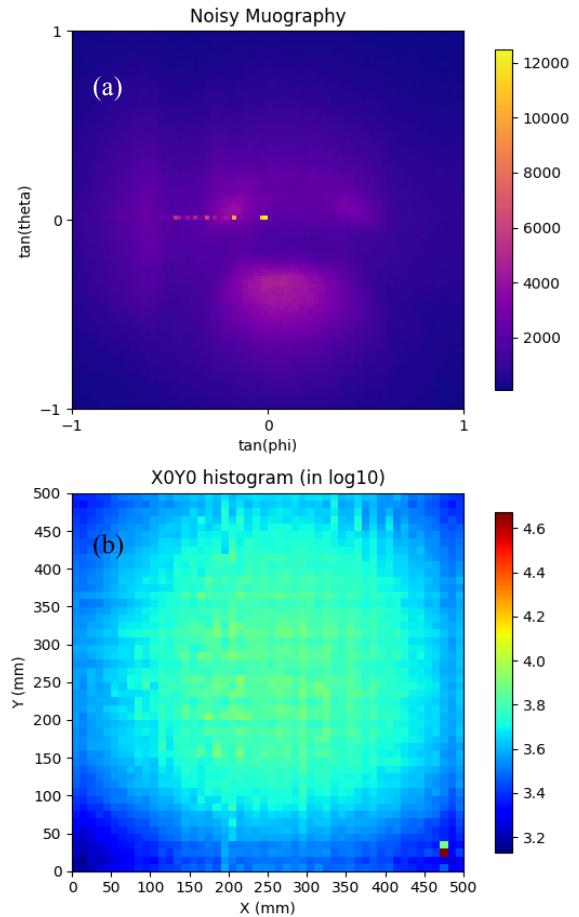


Fig. 10. Muography (a) and associated X0Y0 histogram (b). Noisy pixels appear on the muography and one pixel in the X0Y0 histogram is highly activated.

It is worth mentioning that this method does not bias directly the muography. Indeed, in the muography pixels correspond to direction in space, but the regions filtered correspond to positions on a detector. It means that even if we filter some areas on the detector, the direction in space can still be observed the same way. To study the impact of filtering areas of the detector we observed the effect of a very conservative case. In Fig. 11 half of the detector is filtered (compared to less than 1% normally). We then display the muography using only one half of the detector, and the ratio between this muography and the original muography (with the full detector). This examples demonstrates that even with a half detector it is still possible to have similar muographies.

However Fig. 11 shows a correlation between the directions (on the muography) and the hit positions (on the X0Y0 histogram). Indeed muons coming at high angles tends to hit the detector on the opposite edge. That is why when we filter half of the detector, the muography loses some events on the opposite side (red area on the ratio plot of Fig. 11).

This effect is normally negligible because during the denoising process, less than 1% of the detector surface is filtered. This filtering is then very selective and allows to remove noise with a negligible impact on the muography.

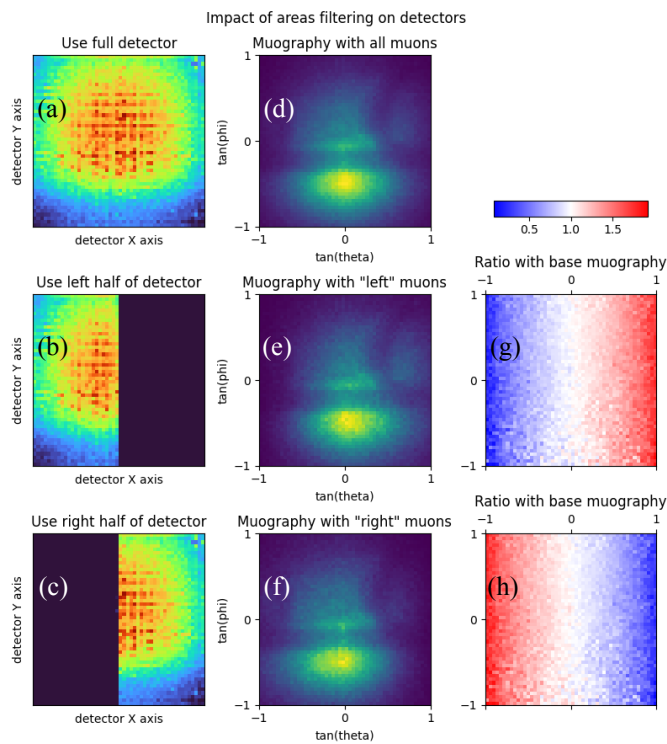


Fig. 11. Left row (a, b, c) shows X0Y0 histogram with filtered areas. The center row (e, f, g) shows the consequences on the related muography. The effect is mainly a loss of muons on one side, which is visible in the ratios in the right row (g, h).

## V. CONCLUSION

Thanks to the experience acquired during the G2 proof of concept, we have developed methods and tools to realize more efficient measurements campaigns.

For the G3 reactor, in the scope of a PhD work, we ran simulations to help us focus on the graphite core. We were able to take data on 46 different positions. Some of those positions were accessible thanks to new mechanical developments.

To process this large amount of data, we also started to automate the different steps between the raw data (hits on the Micromegas detectors) and the opacity computations. We focused on the automation of the most time consuming tasks, like the denoising of the data.

Finally we now have the data and tools to realize the 3D reconstruction of the G3 reactor, which is expected in the next year.

## REFERENCES

- [1] K. Morishima, M. Kuno, A. Nishio et al, "Discovery of a big void in Khufu's Pyramid by observation of cosmic-ray muons.", *Nature*, vol. 552, pp. 386–390, 2017, 10.1038/nature24647.
- [2] S. Procureur, K. Morishima, M. Kuno et al, "Precise characterization of a corridor-shaped structure in Khufu's Pyramid by observation of cosmic-ray muons.", *Nat Commun* vol. 14, no. 1144, 2023, 10.1038/s41467-023-36351-0.

- [3] IAEA, "Muon Imaging Present Status and Emerging Applications", [online]. Available : <https://www-pub.iaea.org/MTCD/Publications/PDF/TE-2012web.pdf>.
- [4] R. Kaiser, "Muography:overview and future directions.", *Phil. Trans. R. Soc. A.*, vol. 377, no. 20180049, 10.1098/rsta.2018.0049.
- [5] A.H. Andersen, A.C. Kak, "Simultaneous Algebraic Reconstruction Technique (SART): A superior implementation of the ART algorithm,", *Ultrasonic Imaging*, vol. 6, no. 1, pp 81-94, 1984, 10.1016/0161-7346(84)90008-7.
- [6] S. Procureur et al, "3D imaging of a nuclear reactor using muography measurements", *Science Advances*, vol. 9, no. 5, 2023, 10.1126/sciadv.abq8431.
- [7] S. Bouteille et al, "A Micromegas-based telescope for muon tomography: The WatTo experiment,", *Nuclear Instruments and Methods in Physics Research Section A*, vol. 834, pp. 223-228, 2016, 10.1016/j.nima.2016.08.002.
- [8] S. Procureur, R Dupre, S. Aune, "Genetic multiplexing and first results with a 50x50 cm2 Micromegas", *Nuclear Instruments and Methods in Physics Research Section A*, vol. 729, pp. 888-894, 2013, 10.1016/j.nima.2013.08.071.
- [9] B. Lefevre, "Convolutional neural networks demultiplexing in large Micromegas detectors for muography purposes", *Machine learning workshop IN2P3-IRFU, 2022*, [online], available : <https://webcast.in2p3.fr/video/convolutional-neural-networks-demultiplexing-in-large-micromegas-detectors-for-muography-purposes>.
- [10] H. Gomez Maluenda, L. Gallego, S. Procureur, "Muography is present at the heart of nuclear reactors", 2020, [online] available : [https://irfu.cea.fr/en/Phoce/Vie\\_des\\_labos/Ast/ast.php?te=fait\\_marquant&id\\_ast=4888](https://irfu.cea.fr/en/Phoce/Vie_des_labos/Ast/ast.php?te=fait_marquant&id_ast=4888).